Title
Outward-facing conformers of LacY stabilized by nanobodies

Journal
Proceedings of the National Academy of Sciences of the United States of America, 111(52)

ISSN
0027-8424

Authors
Smirnova, Irina
Kasho, Vladimir
Jiang, Xiaoxu
et al.

Publication Date
2014-12-30

DOI
10.1073/pnas.1422265112

Peer reviewed

Outward-facing conformers of LacY stabilized by nanobodies

Irina Smirnova[a], Vladimir Kasho[a], Xiaoxu Jiang[a], Els Pardon[b,c], Jan Steyaert[b,c,1], and H. Ronald Kaback[a,d,e,1]

[a]Department of Physiology, [d]Department of Microbiology, Immunology, and Molecular Genetics, and [e]Molecular Biology Institute, University of California, Los Angeles, CA 90095-7327; [b]Structural Biology Research Center, VIB, Pleinlaan 2, 1050 Brussels, Belgium; and [c]Structural Biology Brussels, Vrije Universiteit Brussel, Pleinlaan 2, 1050 Brussel, Belgium

Contributed by H. Ronald Kaback, November 21, 2014 (sent for review October 31, 2014)

The lactose permease of *Escherichia coli* (LacY), a highly dynamic polytopic membrane protein, catalyzes stoichiometric galactoside/H^+ symport by an alternating access mechanism and exhibits multiple conformations, the distribution of which is altered by sugar binding. We have developed single-domain camelid nanobodies (Nbs) against a LacY mutant in an outward (periplasmic)-open conformation to stabilize this state of the WT protein. Twelve purified Nbs inhibit lactose transport in right-side–out membrane vesicles, indicating that the Nbs recognize epitopes on the periplasmic side of LacY. Stopped-flow kinetics of sugar binding by WT LacY in detergent micelles or reconstituted into proteoliposomes reveals dramatic increases in galactoside-binding rates induced by interaction with the Nbs. Thus, WT LacY in complex with the great majority of the Nbs exhibits varied increases in access of sugar to the binding site with an increase in association rate constants (k_{on}) of up to ∼50-fold (reaching 10^7 $M^{-1}{\cdot}s^{-1}$). In contrast, with the double-Trp mutant, which is already open on the periplasmic side, the Nbs have little effect. The findings are clearly consistent with stabilization of WT conformers with an open periplasmic cavity. Remarkably, some Nbs drastically decrease the rate of dissociation of bound sugar leading to increased affinity (greater than 200-fold for lactose).

membrane transport proteins | fluorescence | major facilitator superfamily

Typical of many transport proteins, from organisms as widely separated evolutionarily as *Archaea* and *Homo sapiens*, the lactose permease of *Escherichia coli* (LacY), a paradigm for the Major Facilitator Superfamily (1), catalyzes the coupled, stoichiometric translocation of a galactopyranoside and an H^+ (galactoside/H^+ symport) across the cytoplasmic membrane (reviewed in refs. 2 and 3). Although it is now generally accepted that membrane transport proteins operate by an alternating access mechanism, this has been documented almost exclusively for LacY (reviewed in refs. 4 and 5). By this means, galactoside- and H^+-binding sites become alternatively accessible to either side of the membrane as the result of reciprocal opening/closing of cavities on the periplasmic and cytoplasmic sides of the molecule. LacY is highly dynamic, and alternates between different conformations (6, 7).

Until recently, six X-ray structures of LacY have exhibited the same inward-facing conformation with an aqueous cavity open to the cytoplasmic side, a tightly sealed periplasmic side, and sugar- and H^+-binding sites in the middle of the molecule (8–11). Numerous studies confirm that this conformation prevails in the absence of sugar (12–16). Recently, however, the X-ray structure of double-Trp mutant G46W/G262W with bound sugar reveals a conformation with a narrowly open periplasmic pathway and a tightly sealed cytoplasmic side (PDB ID code 4OAA) (17), thereby providing structural evidence that an intermediate occluded conformation occurs between the outward- and inward-facing conformations in the transport cycle.

Rates of opening/closing of periplasmic and cytoplasmic cavities have been determined in real time from changes in fluorescence of Trp or attached fluorophores with LacY either in detergent micelles or in reconstituted proteoliposomes (PLs) (15, 18, 19). Sugar-binding rates with WT LacY in PLs measured by Trp151→4-nitrophenyl-α-D-galactopyranoside (NPG) FRET are independent of sugar concentration, whereas the mutant with an open periplasmic cavity is characterized by a linear concentration dependence of sugar binding rates with k_{on} of ∼10 $\mu M^{-1}{\cdot}s^{-1}$ (18, 20), which approximates diffusion controlled access to the binding site (21). Therefore, with WT LacY embedded in PLs, the periplasmic side is sealed, and substrate binding is limited by opening of the periplasmic cavity at a rate of 20–30 s^{-1} (19). This rate is very similar to the turnover number of WT LacY in right-side–out (RSO) membrane vesicles or reconstituted PLs (22) and is consistent with the notion that opening of the periplasmic cavity may be a limiting step in the overall transport mechanism.

To define and characterize partial reactions in the LacY transport cycle, stable conformers would be particularly useful. In this regard, remarkable progress has been made with G protein-coupled receptors through the use of camelid single-domain nanobodies (Nbs), which stabilize specific conformers (23–27). Advantages of Nbs include small size and a unique structure that allows flexible antigen-binding loops to insert into clefts and cavities. Here we report that Nbs prepared against the outward (periplasmic)-open LacY mutant G46W/G262W effectively bind to WT LacY and inactivate transport activity. However, the sugar-binding site becomes much more accessible to galactosides as a result of Nb binding, indicating stabilization of the open-outward conformations of LacY, and providing the means for detailed studies of galactoside binding to these conformers. Remarkably, several Nbs significantly increase affinity for galactosides by slowing the dissociation rate of the sugar while maintaining a high association rate. It is also apparent that the

Significance

LacY, a paradigm for the major facilitator superfamily (the largest family of transport proteins) catalyzes the coupled symport of a galactoside and an H^+. Although a detailed mechanism has been postulated, to test its veracity stable conformers of different intermediates would be particularly informative. Camelid single-domain nanobodies (Nbs), which can stabilize specific conformers, are ∼15 kDa in size and have a unique structure that allows flexible antigen-binding loops to insert into clefts and cavities. Nbs prepared against an outward (periplasmic)-open LacY mutant are described herein. The Nbs bind effectively to WT LacY and inactivate transport by stabilizing the symporter in outward-open conformations with increased accessibility to the sugar-binding site. Moreover, several Nbs dramatically increase affinity for galactosides.

Author contributions: I.S., V.K., J.S., and H.R.K. designed research; I.S., V.K., X.J., E.P., and J.S. performed research; I.S., V.K., E.P., and J.S. contributed new reagents/analytic tools; I.S., V.K., X.J., E.P., and H.R.K. analyzed data; and I.S., V.K., E.P., J.S., and H.R.K. wrote the paper.

The authors declare no conflict of interest.

[1]To whom correspondence may be addressed. Email: jan.steyaert@vub.ac.be or rkaback@mednet.ucla.edu.

This article contains supporting information online at www.pnas.org/lookup/suppl/doi:10.1073/pnas.1422265112/-/DCSupplemental.

Nbs have the potential for crystallizing LacY trapped as otherwise unstable transient intermediates.

Results

Generation of Nbs. To generate Nbs that recognize and stabilize outward-open conformations of LacY, llamas were immunized (28) with LacY mutant G46W/G262W (20) reconstituted into PLs as the antigen. In this mutant, double-Trp replacements for Gly46 (helix II) and Gly262 (helix VIII) were introduced on the periplasmic side of LacY at positions where the two six-helix bundles come into close contact. Introduction of bulky Trp residues at these positions prevents closure of the periplasmic cavity and completely abrogates all transport activity. The double-Trp mutant reconstituted into PLs is oriented physiologically, with the periplasmic side facing the external medium (20), as demonstrated previously (18, 29). Thus, it is presumed that the llama's immune system is presented with an antigen that has an accessible periplasmic surface of LacY with an open cavity. Selections were performed on the LacY mutant to find those nanobodies that would specifically recognize the outward-open conformation, as well as on WT LacY. Procedures used for production, selection, cloning, and purification of Nbs are provided in *Methods*.

Lactose Transport. Lactose/H^+ symport catalyzed by WT LacY was measured in RSO membrane vesicles preincubated with each of 13 nanobodies, and the data are summarized in Table 1 and Fig. S1. Nb 9051 has no significant effect on the rate of lactose transport, but Nb 9042, Nb 9035, and Nb 9034 inhibit by 60%, 80%, and 90%, respectively, and other nine Nbs block lactose transport completely. Because it is well known that vesicles prepared by osmotic lysis of spheroplasts have the same orientation as the membrane in intact cells (for examples, see refs. 30 and 31–34), the results demonstrate that inhibition of transport by the Nbs is specifically a result of binding epitopes on the periplasmic side of WT LacY.

Sugar Binding to Nb/LacY Complexes. Sugar binding rates were measured by Trp151→NPG FRET with WT LacY or the double-Trp mutant solubilized in *n*-dodecyl-β-D-maltopyranoside (DDM) by using stopped-flow fluorimetry, which allows determination of association and dissociation rate constants (k_{on} and k_{off}) of sugar binding. WT LacY exhibits a k_{on} of 0.2 $\mu M^{-1}\cdot s^{-1}$, whereas k_{on} for the double-Trp mutant is 5.7 $\mu M^{-1}\cdot s^{-1}$ (compare open circles in Fig. 1*A* with open diamonds in Fig. 1*B*), indicating much higher accessibility of the sugar-binding site in mutant G46W/G262W with an open periplasmic cavity. None of Nbs tested abolish sugar binding to LacY (Table 1). Two Nbs (9051 and 9035) practically do not affect sugar binding (k_{on} and k_{off} values are similar to those measured for WT LacY without Nbs). Interaction of Nb 9042 and Nb 9034 with WT LacY results in sugar binding with rates independent of NPG concentration (k_{obs} = 30 and 15 s^{-1}, respectively), suggesting that these two nanobodies do not alter galactoside binding. Rather, they may decrease conformational flexibility of LacY in such a manner that sugar access to the binding site is limited by a slow conformational change or slow opening of the periplasmic cavity, which could explain partial inhibition of transport.

Nine Nb /WT LacY complexes that completely block transport, demonstrate a significant increase of NPG binding rates (k_{on} increases from 5- to 50-fold) (Fig. 1*A* and Table 1). Dramatic increases in NPG accessibility are observed for WT LacY complexed with Nbs 9039, 9048, 9047, 9033, and 9065 to an extent comparable to that of mutant G46W/G262W (Table 1) (k_{on} = 4.4, 6.8, 6.9, 7.5, and 9.3 $\mu M^{-1}\cdot s^{-1}$, respectively). Several Nbs exhibit a smaller effect on the rates of sugar binding by WT LacY, with k_{on} values of 1.0, 1.2, 3.5, and 3.5 $\mu M^{-1}\cdot s^{-1}$ for Nbs 9036, 9055, 9063, and 9043, respectively (Fig. 1*A* and Table 1). Notably, the double-Trp mutant in complex with Nbs 9036, 9063, and 9043 is characterized by lower k_{on} values than observed without Nbs, whereas all other Nbs have essentially no effect (Fig. 1*B* and Table 1). Kinetic parameters measured by displacement of bound NPG using a high concentration of β-D-galactopyranosyl-1-thio-β-D-galactopyranoside (TDG) show that the majority of the Nbs, which block transport, significantly increase the affinity of WT LacY for NPG (K_ds decrease up to 10 times), whereas K_ds are mostly unaltered with the double-Trp mutant (Table 1, shaded columns). Surprisingly, similar effects of Nb 9036 are observed with both WT LacY, and mutant G46W/

Table 1. Effect of Nbs on lactose transport and kinetics of sugar binding to LacY

	WT LacY				G46W/G262W LacY		
			Displacement			Displacement	
Nb	Lactose transport (%)	Binding k_{on} ($\mu M^{-1}\cdot s^{-1}$)	k_{off} (s^{-1})	K_d (μM)	Binding k_{on} ($\mu M^{-1}\cdot s^{-1}$)	k_{off} (s^{-1})	K_d (μM)
None	100	0.2	41	28	5.7	31	6.1
9051	100	0.2	48				
9042	40	ND*	41				
9035	20	0.3	24				
9034	10	ND*	38	60	8.6	34	5.7
9036	No	1.0	0.05	0.05†	0.3	0.02	0.07†
9055	No	1.2	52	35	4.1	63	18
9063	No	3.5	2.7	2.2	1.2	1.4	3.3
9043	No	3.0	8	4	2.2	4.8	3.2
9039	No	4.4	54	13	5.3	45	18
9048	No	6.8	13	2.8	4.4	11	4.2
9047	No	6.9	32	5.2	5.8	31	3.8
9033	No	7.5	31	3.8	5.3	29	5.2
9065	No	9.3	40	5.3	9.5	58	9.1

Rates of lactose transport were measured as described in *Methods* and Fig. S1. Rates of NPG binding were measured as Trp151→NPG FRET by stopped-flow fluorimetry (*Methods*). Association rate constants (k_{on}) were measured as described in Figs. 1 and 2. Dissociation rate constants (k_{off}) and K_d values were measured in displacement experiments (data in shaded columns), as shown in Fig. S2. Statistical SDs were within 10% for each presented data point. Color coding is the same as in Figs. 1 and 2. Only those Nbs that completely block transport in WT LacY were tested with the double-Trp mutant.

*Binding rates do not change with NPG concentration.

†K_d values for Nb9036/LacY complexes were calculated (k_{off}/k_{on}).

BIOCHEMISTRY

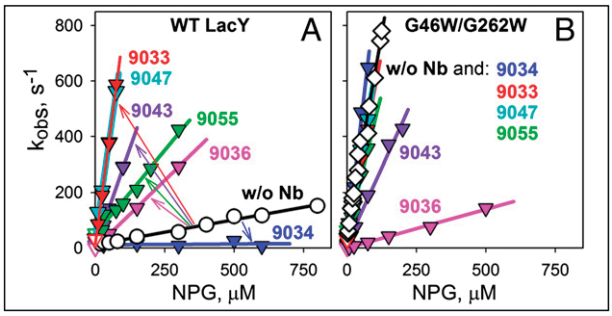

Fig. 1. Effect of six Nbs on kinetics of sugar binding by WT LacY (*A*) or mutant G46W/G262W (*B*) solubilized in DDM. Stopped-flow rates of NPG binding (k_{obs}) were measured by mixing LacY with NPG in the absence or presence of a given Nb. Stopped-flow traces of the decrease in Trp fluorescence were recorded and fitted with single-exponential equation for estimation of the sugar-binding rate (k_{obs}) at each NPG concentration. Concentration dependencies of k_{obs} for NPG binding to proteins without Nbs are shown in black (open circles, WT LacY; and open diamonds, double-Trp mutant). Data obtained with different Nbs are shown in the same colors as in Table 1. The slopes of the linear concentration dependencies of NPG binding rates ($k_{obs} = k_{off} + k_{on}$[NPG]) yielded the k_{on} values presented in Table 1 in the columns labeled "Binding." The arrows in *A* indicate the effect of each Nb on the accessibility of the sugar-binding site relative to WT LacY with no Nb.

G262W where NPG binding affinity is increased by orders of magnitude, which will be discussed in detail below.

Accessibility of the Sugar-Binding Site. Remarkable changes in sugar-binding rates are induced by interaction of Nb 9065 with WT LacY (Fig. 2*A* and Table 1). As estimated from the linear concentration dependence of binding rates, k_{on} increases from 0.2 to 9.3 $\mu M^{-1}\cdot s^{-1}$ (Fig. 2*B*), indicating free access to the sugar-binding site. Moreover, NPG binding rates are the same when the LacY/Nb 9065 complex is formed in the absence or presence of sugar (Fig. 2*B*, red triangles). WT LacY binding affinity for NPG is significantly increased by interaction with Nb 9065 (Table 1). The K_d value measured in displacement experiments decreases from 28 to 5.3 μM (Fig. S2 *A*, *C*, and *E*). Nb 9065 does not markedly alter NPG-binding kinetics with the G46W/G262W mutant (Fig. 2*B*, Table 1, and Fig. S2 *B*, *D*, and *F*).

Experiments with LacY solubilized in DDM do not specify whether Nb binding stabilizes conformers with an open periplasmic or cytoplasmic cavity. However, LacY reconstituted into PLs is oriented with the periplasmic side facing out, as in the native *E. coli* membrane (18, 20, 29). Therefore, a kinetic test was designed that allows discrimination between accessibility from the periplasmic or cytoplasmic sides of LacY by comparing sugar-binding rates with LacY solubilized in DDM versus reconstituted into PLs (Fig. S3). Mutants G46W/G262W or C154G with an open periplasmic or cytoplasmic cavity, respectively, are characterized by rapid sugar binding in DDM (Fig. S3 *A* and *D*) (k_{on} = 5 $\mu M^{-1}\cdot s^{-1}$). However, in PLs, sugar binding by mutant G46W/G262W is rapid and demonstrates a sharp concentration dependence of k_{obs} (with k_{on} = 14 $\mu M^{-1}\cdot s^{-1}$), whereas mutant C154G exhibits a relatively slow rate of sugar binding that is independent of galactoside concentration (k_{obs} = 50 s^{-1}) (Fig. S3 *B* and *E*). Thus, NPG has free access to the binding site from periplasmic side in the double-Trp mutant, but limited access in mutant C154G, where the rate of opening of the periplasmic cavity is limiting. However, k_{on} determined by displacement with reconstituted mutant C154G in PLs (Fig. S3*F*) (k_{on} = 14 $\mu M^{-1}\cdot s^{-1}$) is even higher than in DDM (k_{on} = 4.9 $\mu M^{-1}\cdot s^{-1}$). Thus, when the periplasmic cavity is open, the sugar binds with a diffusion-controlled rate.

Binding of NPG by WT LacY in DDM is characterized by k_{on} = 0.2 $\mu M^{-1}\cdot s^{-1}$ and consistent with reduced access to the sugar binding site (Fig. S3*G*). NPG binding by WT LacY reconstituted into PLs is slow (k_{obs} = 21 s^{-1}), and the rate is independent of sugar concentration, thereby indicating that binding is limited by opening of the periplasmic cavity (Fig. S3*H*). However, in displacement experiments with reconstituted WT LacY, opening of periplasmic cavity provides free access to binding site with a k_{on} of 10 $\mu M^{-1}\cdot s^{-1}$ (Fig. S3*I*), as shown for mutant C154G.

Binding of Nb 9065 to reconstituted WT LacY dramatically increases NPG binding rates, but no significant change is observed with the reconstituted double-Trp mutant (Fig. 2*C*). Linear fits of the data yield an estimated k_{on} of ~20 $\mu M^{-1}\cdot s^{-1}$ for both WT LacY and mutant G46W/G262W complexed with Nb 9065. Therefore, Nb 9065 binds to an epitope on reconstituted WT protein that is exposed to the external milieu, provides free access of NPG to the binding site, and blocks transport, thereby demonstrating clearly that Nb 9065 stabilizes an outward-facing conformer of WT LacY. Similar effects of Nb 9039 and 9047 on reconstituted WT LacY and of Nbs 9043, 9047 and 9065 on reconstituted mutant C154G are shown in Fig. S4.

Nb 9036 Induces High-Affinity Galactoside Binding. A striking effect of Nb 9036 on sugar binding is observed with both WT LacY and the double-Trp mutant. True k_{off} values for NPG determined in displacement experiments decrease in the presence of Nb 9036 by about three orders-of-magnitude from 41 to 0.05 s^{-1} and from 31 to 0.02 s^{-1} for the WT and mutant, respectively (Table 1). With the WT LacY/Nb 9036 complex, NPG binding rates increase (Fig. S5*A*), demonstrating greater accessibility of the sugar-binding site (k_{on} increases fivefold) (Fig. 1*A* and Table 1). Displacement rates are greatly decreased by Nb 9036 binding to WT LacY (Fig. S5*B*), resulting in a >500-fold increase in NPG affinity. A similar effect of Nb 9036 is observed with mutant G46W/G262W, although both k_{on} and k_{off} values are decreased (Table 1). Therefore, it appears that Nb 9036 binding stabilizes a specific outward-facing conformation of LacY in which the periplasmic cavity is partially open, but release of bound NPG is drastically hindered.

This effect of Nb 9036 allows characterization of the kinetic properties of lactose binding, the physiological substrate of LacY. The affinity of LacY for lactose in the absence of Nbs is extremely low with a K_d of ~10 mM (35, 36). The rate of lactose displacement was measured by Trp151→NPG FRET, where

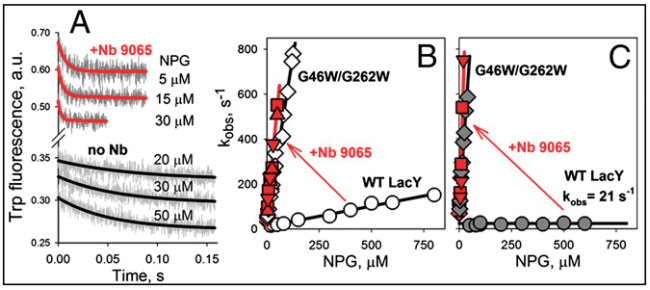

Fig. 2. Effect of Nb 9065 on accessibility of the sugar-binding site. NPG binding rates were measured directly by stopped-flow as Trp151→NPG FRET with WT LacY and G46W/G262W mutant in the absence of Nbs (black lines) or after preincubation with Nb 9065 (red lines). (*A*) Stopped-flow traces of Trp emission decreases were recorded with WT LacY in DDM after mixing with given concentrations of NPG. (*B*) Concentration dependencies of sugar binding rates measured in DDM with WT LacY (open circles and red triangles) or mutant (open diamonds and red squares). WT LacY preincubated with Nb 9065 in the absence or presence of sugar (red triangles pointed down or up, respectively) exhibits the same NPG binding rates. Estimated k_{on} values are presented in Table 1 in columns labeled "Binding." WT LacY/Nb 9065 complex in DDM solution exhibits ~50-fold increase in k_{on} (from 0.20 ± 0.01 to 9.3 ± 0.2 $\mu M^{-1}\cdot s^{-1}$). (*C*) Concentration dependencies of sugar binding rates measured with WT LacY (gray circles or red triangles) and mutant (gray diamonds and red squares) reconstituted into PLs. The red arrows indicate the change in concentration dependence of sugar binding rates after Nb 9065 binding to WT LacY.

a saturating concentration of NPG (0.2 mM) was mixed with WT LacY/Nb 9036 complex preincubated with given concentrations of lactose (Fig. 3*A*). The stopped-flow traces demonstrate that NPG binding occurs upon release of lactose at constant rate ($k_{off} = 1.8\ s^{-1}$). As estimated from the concentration dependence of the amplitudes of the fluorescence change (Fig. 3*B*), the K_d for lactose is 42 μM. The double-Trp mutant complexed with Nb 9036 yields a similar K_d of 49 μM (Fig. 3*B*), suggesting that Nb 9036 stabilizes similar conformers of both proteins.

Nbs Binding. Homology modeling of the 3D structures of each Nb described reveals Trp residues in the variable loops containing the complementarity determining regions (CDRs) that define the binding affinity of the Nbs (Fig. 4*A*). Therefore, interaction of the Nbs with LacY was studied by site-directed Trp-induced fluorescence quenching of bimane- or ATTO655-labeled LacY (19, 37, 38). WT LacY with a Cys replacement on the periplasmic side (I32C) labeled with bimane or ATTO655 exhibits a decrease in the fluorescence emission of either fluorophore upon addition of Nbs (Fig. S6). Time-courses of the fluorescence changes recorded with bimane-labeled (Fig. 4*B*) or ATTO655-labeled (Fig. 4*C*) mutant I32C LacY demonstrate various extents of fluorescence quenching after addition of Nbs 9036, 9055, and 9063, which likely reflect different distances between the Trp residues in the Nbs and the fluorophores in LacY when the Nb binds.

Stopped-flow mixing of various concentrations of Nb with 0.4 μM bimane-labeled LacY (Fig. S7) exhibits increased rates of binding with increasing Nb concentration. No change in the amplitude of the fluorescence decrease is observed even at lowest Nb concentrations (0.5–1 μM), which indicates that the affinity of Nbs for LacY is high with K_d values at least in the nanomolar range. Linear concentration dependencies of Nbs binding rates (Fig. 5) yield estimated k_{on} values that vary from 0.2 to 3.5 $\mu M^{-1}{\cdot}s^{-1}$, and extremely low k_{off} values for all five Nbs. In addition, the binding rates of Nb 9036 to bimane-labeled I32C LacY are identical in the absence or presence of 5 mM TDG ($k_{on} = 0.4\ \mu M^{-1}{\cdot}s^{-1}$), indicating that Nb recognizes the same LacY conformer with or without bound sugar.

When the Cys replacement is introduced on the cytoplasmic side of WT LacY (S401C), no significant Trp-induced fluorescence quenching is observed with bimane- or ATTO655-labeled LacY upon Nb binding (Fig. S8 *A*–*C*), although the effect of Nb 9036 on NPG binding kinetics for bimane-labeled S401C LacY is readily detected (Fig. S8*D*). In the bimane-labeled S401C LacY/Nb 9036 complex, both k_{on} and k_{off} values are altered to the same extent as observed with WT LacY/Nb 9036. Thus, the Nbs bind to the periplasmic side of LacY in DDM, and the method allows determination of Nb binding kinetics with LacY.

Binding affinity of Nb 9036, Nb 9055, or Nb 9063 was measured by steady-state titration of bimane- or ATTO655-labeled I32C LacY at low protein concentration (20 nM). Estimated K_d values for all three Nbs are around 1 nM and do not depend on the structure of fluorophore attached to LacY (Fig. S9). The presence of sugar practically does not change Nbs binding affinity. Measured k_{on} (Fig. 5) and K_d values allow calculation of k_{off} as 1.2×10^{-3}, 0.4×10^{-3}, and $0.3 \times 10^{-3}\ s^{-1}$ for dissociation of Nbs 9063, 9055, and 9036, respectively.

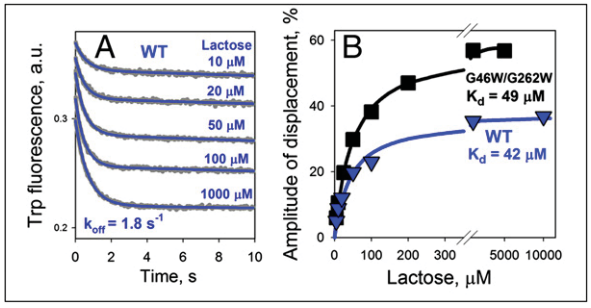

Fig. 3. Lactose binding affinity of WT LacY or mutant G46W/G262W complexed with Nb 9036. LacY/Nb complexes solubilized in DDM were preincubated with indicated concentrations of lactose and then mixed by stopped-flow with a saturating concentration of NPG (0.2 mM) that binds upon release of ligand and is an acceptor of FRET from Trp151. Binding of NPG to sugar-free protein is fast with observed rate estimated as ~200 s^{-1}. This rate is much faster than the lactose dissociation rate, and only the displacement rate for lactose (k_{off}) is measured. (*A*) Time traces of Trp fluorescence change were recorded with the WT LacY/Nb 9036 complex and fitted with a single-exponential equation (blue lines) that yield estimated rates of lactose dissociation ($k_{off} = 1.8 \pm 0.2\ s^{-1}$) by displacement with NPG. (*B*) Affinity of lactose binding was estimated from hyperbolic fits of the concentration dependence of the fluorescence changes at each lactose concentration in the stopped-flow traces for WT and mutant (triangles and squares, respectively). K_d values are 42 ± 5 and 49 ± 2 μM for the WT LacY and mutant complexes, respectively.

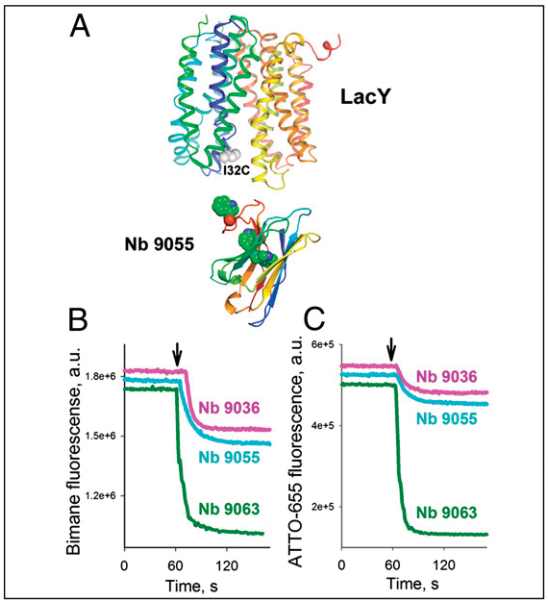

Fig. 4. Nb binding to periplasmic LacY I32C mutant labeled with fluorophores. Structural models of LacY and Nb 9055 (*A*) are shown as rainbow colored backbones (from blue to red) with highlighted Trp residues in the Nb (green spheres) and introduced Cys32 on periplasmic side of LacY (gray spheres) (PDB ID code 4OAA). Time courses of fluorescence quenching were recorded at excitation/emission wavelengths of 380/465 nm or 660/677 nm for bimane or ATTO655, respectively. Addition of 0.6 μM Nb 9036, Nb 9055, or Nb 9063 to 0.3 μM I32C LacY mutant labeled with bimane-maleimide (*B*) or ATTO655-maleimide (*C*) is indicated by black arrows. The effects of the Nbs on the emission spectra of fluorophore-labeled LacY are shown in Fig. S6.

Demonstration That Nb Binding Stabilizes a Conformer with an Open Periplasmic Cavity. Trp-induced bimane unquenching allows direct demonstration of opening of periplasmic cavity in LacY (19). Thus, bimane-labeled mutant F29W/G262C exhibits unquenching of bimane fluorescence after addition of sugar, indicating opening of the periplasmic cavity and even greater unquenching is observed after addition of Nb 9036 (Fig. 6*A*). The increased extent of bimane fluorescence unquenching caused by Nb binding compared with effect of TDG is most likely explained by stabilization of a specific outward-open conformation of LacY, whereas sugar binding results in dynamic equilibrium of several LacY conformers including those with an open periplasmic cavity (6). Furthermore, the rates of unquenching measured with bimane-labeled F29W/G262C at increasing concentrations of Nb 9036 exhibit a linear dependence with $k_{on} = 0.4\ \mu M^{-1}{\cdot}s^{-1}$ (Fig. 6*B*). This k_{on} value is identical to that measured by direct binding studies with Nb 9036 by using Trp-induced quenching of bimane-labeled I32C LacY (Fig. 5, pink circles), thereby demonstrating that binding of Nb 9036 stabilizes a conformer with an open periplasmic cavity.

BIOCHEMISTRY

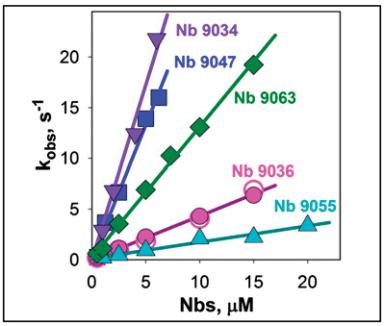

Fig. 5. Kinetics of Nbs binding to LacY. Rates of Nbs binding to bimane-labeled mutant I32C LacY were measured by stopped-flow as quenching of bimane fluorescence by Trp residues of the five Nbs indicated. Data were obtained with 0.4 μM LacY as described in Fig. S7. The linear dependencies of the observed rates on Nb concentrations yield estimated k_{on} values of 0.16 ± 0.01, 0.43 ± 0.01, 1.30 ± 0.02, 2.7 ± 0.1, and 3.5 ± 0.2 $\mu M^{-1}{\cdot}s^{-1}$ for Nbs 9055, 9036, 9063, 9047, and 9034, respectively. Nb 9036 binding rates were measured in the absence or presence of 5 mM TDG (open and closed pink circles, respectively).

Discussion

Nbs represent a unique type of single-domain antibodies with flexible antigen-binding loops containing CDR3, which is able to insert into clefts and cavities of membrane proteins and stabilize specific conformers (23–27). Therefore, Nbs were prepared against LacY mutant G46W/G262W, which is in an outward-open conformation, anticipating that such Nbs would interact with epitopes within the open periplasmic cavity to stabilize outward-facing conformers of WT LacY. As shown, 12 of the 13 Nbs characterized inhibit—and 9 totally block—lactose transport catalyzed by WT LacY in RSO membrane vesicles, indicating that they bind to periplasmic epitopes. However, sugar binding is not abolished. Rather, each of the nine Nbs significantly increases the rate of sugar binding with WT LacY solubilized in DDM, indicating that the sugar-binding site in the middle of the LacY molecule becomes much more accessible to the external medium in the presence of the Nbs. Even more impressive, WT LacY and C154G mutant reconstituted into PLs and then exposed to Nbs 9039, 9043, 9047, and 9065 exhibit virtually unrestricted sugar binding rates with high k_{on} values corresponding to stabilization of conformers with an open periplasmic cavity. It is also remarkable that with few exceptions (Nbs 9036, 9063, and 9043), the Nbs have little or no effect on sugar-binding rates with the double-Trp mutant presumably because the mutant is already open on the periplasmic side.

Although Nb binding to WT LacY generally increases accessibility of the binding site to NPG, the k_{on} values vary from 1 to 9 $\mu M^{-1}{\cdot}s^{-1}$ for different WT LacY/Nb complexes. Thus, the Nbs appear to recognize different epitopes and stabilize different outward-open conformers of LacY that may represent natural intermediates in the transport cycle.

Remarkably, three of the Nbs (9036, 9063, and 9043) significantly decrease k_{off} values measured for NPG with WT LacY/Nb complexes, and dissociation of sugar is slowed nearly 1,000-fold by Nb 9036 (Table 1), resulting in markedly increased affinity for galactosides. Thus, the K_d value of the Nb 9036/WT LacY complex for NPG decreases by >500-fold. This huge increase in affinity for galactoside allows determination of binding kinetics for lactose, the natural substrate of LacY where affinity increases >200-fold. Because Nb 9036 also decreases k_{off} and k_{on} values in complex with the double-Trp mutant to near those observed for WT LacY/Nb 9036 complex, it seems reasonable to suggest that this Nb stabilizes a conformer that approximates an occluded intermediate with fully liganded sugar.

A simple fluorescent method was developed for detection of Nb binding to LacY by using site-directed Trp-induced quenching of a fluorophore attached to the periplasmic side of LacY. Quenching of the fluorophore introduced on the periplasmic but not on cytoplasmic side of LacY also confirms that the Nbs bind to epitopes on the periplasmic side of LacY. Moreover, presteady-state kinetics of Nb binding to LacY were measured by stopped-flow. The linear concentration dependencies of binding rates reveal significant variations in k_{on} values for five tested Nbs (from 0.2 to 3.5 $\mu M^{-1}{\cdot}s^{-1}$) and exceedingly low k_{off} values. Multiple k_{on} values most likely correspond to interaction of the Nbs with different epitopes on periplasmic side of LacY that vary in complexity and structure. Binding affinities measured by steady-state titration are very high (K_d values are around 1 nM for Nbs 9036, 9055, and 9063), which explains extremely slow dissociation rates of the Nbs. Thus, calculated k_{off} values range from 0.3×10^{-3} to 1.2×10^{-3} s^{-1}, which are similar to published data for highly specific Nbs–antigen interactions (25).

Recognition of different epitopes in WT LacY by the Nbs results in stabilization of several conformational states of the symporter. These states may represent natural functional intermediates in overall transport cycle, as the Nbs do not interfere with sugar binding and therefore with protonation, because effective sugar binding requires the protonated form of LacY (39). Moreover, in vivo-matured Nbs do not apparently induce nonnative conformations of antigens (28). Thus, Nbs developed against the outward-open LacY mutant may be useful for crystallization of WT LacY in different conformations without the use of mutagenesis.

Methods

Construction of mutants, purification of LacY, reconstitution into PLs, and materials used in this study are described in *SI Methods*. All animal vaccination experiments were executed in strict accordance with good animal practices, following the EU animal welfare legislation and after approval of the local ethical committee (Ethical Committee for use of laboratory animals of the Vrije Universiteit Brussel, VUB project 13-601-1). Every effort was made to minimize suffering.

Generation of Nbs. Nbs were prepared against the G46W/G262W LacY mutant using a previously published protocol (28). In brief, one llama (*Lama glama*) received six weekly injections of 100 μg of purified G46W/G262W LacY reconstituted into PLs with lipid to protein ratio 5 (0.4 mg/mL LacY and 2 mg/mL

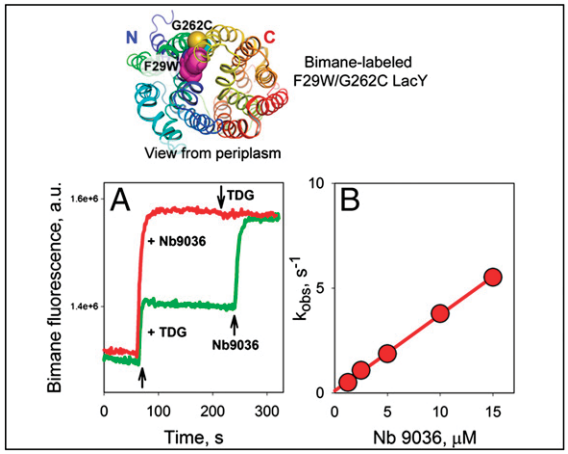

Fig. 6. Stabilizing the open periplasmic cavity by binding of Nb 9036. Structural model of mutant F29W/G262C in inward-facing conformation with a closed periplasmic cavity is shown on top with the backbone rainbow colored (from blue to red) and highlighted Trp- and Cys-replacements (magenta and yellow spheres, respectively) on the periplasmic side of the N- and C-terminal six-helix bundles of LacY. (*A*) Unquenching of fluorescence of bimane-labeled F29W/G262C LacY (0.3 μM) after addition of 5 mM TDG followed by 0.6 μM Nb 9036 (green line), or addition of 0.6 μM Nb 9036 followed by 5 mM TDG (red line). Time courses were recorded as described in Fig. 4*B*. (*B*) Rates of Nb 9036 binding were measured by stopped-flow as described in Fig. 5 by mixing indicated concentrations of Nb 9036 with bimane-labeled F29W/G262C LacY. Unquenching of bimane-labeled Cys262 in LacY results from separation of the fluorophore from Trp29 when the periplasmic cavity opens. Linear concentration dependence of the rates yields an estimated $k_{on} = 0.36 \pm 0.01$ $\mu M^{-1}{\cdot}s^{-1}$.

phospholipids). The Nb-encoding ORFs were amplified from total lymphocyte RNA and subcloned into the phage display/expression vector pMESy4. After one round of panning, clear enrichment was seen for the LacY double-Trp mutant. Ninety-two individual colonies were randomly picked, and the Nbs were produced as soluble His- and Capture Select C-tagged proteins (MW 12–15 kDa) in the periplasm of *E. coli*. Testing for specific binding to both the G46W/G262W mutant and WT LacY (with the fucose transporter as a negative control) resulted in 31 families with the highest signals with mutant G46W/G262W compared with WT LacY. All selections and screenings were done in the absence of sugar. Inducible periplasmic expression of Nbs in *E. coli* WK6 produces milligram quantities of >95% pure nanobody using immobilized metal ion affinity chromatography (Talon resin) from the periplasmic extract of a 1-L bacterial culture. Purified nanobodies (2–10 mg/mL) in 100 mM potassium phosphate (KP_i, pH 7.5) were frozen in liquid nitrogen and stored at –80 °C before use.

Transport Measurements. RSO vesicles for transport assay were prepared from *E. coli* T184 harboring plasmid pT7-5 encoding WT LacY as described in *SI Methods*. The effect of the Nbs on lactose transport was measured after preincubation of vesicles (0.5 mg of total membrane protein) with 80 μg of each Nb (at ~5:1 molar ratio of Nb:LacY) in 100 mM KP_i/10 mM $MgSO_4$ (pH 7.2) for 20 min. Lactose transport was assayed with 0.4 mM [^{14}C]lactose (10 mCi/mmol) in the same buffer at room temperature (see *SI Methods* for details).

Fluorescence Measurements. Stopped-flow measurements were performed at 25 °C on a SFM-300 rapid kinetic system equipped with a TC-50/10 cuvette (dead-time 1.2 ms), and MOS-450 spectrofluorimeter (Bio-Logic). NPG binding was measured as Trp151→NPG FRET at excitation 295 nm with emission interference filters (Edmund Optics) at 340 nm. LacY/Nb complexes were formed by preincubation of purified LacY (20–30 μM) with 1.2 molar excess of each Nb in 50 mM NaP_i/0.02% DDM, pH 7.5 for 10 min at room temperature. Stopped-flow traces were recorded at final concentration 0.5–0.8 μM of LacY after mixing with NPG. In displacement experiments LacY/Nb complex was preincubated with NPG and then mixed with 15 mM TDG in stopped-flow. Measurements with purified protein in DDM were done in 50 mM NaP_i/0.02% DDM (pH 7.5). Experiments with PLs were carried out in 50 mM NaP_i (pH 7.5). To dissolve PLs, DDM was added to a final concentration of 0.3%, and after 10 min, the samples were used in stopped-flow experiments. Typically, 10–30 traces were recorded for each datapoint, averaged and fitted with an exponential equation using the built-in Bio-Kine32 software package or by using Sigmaplot 10 (Systat Software). Calculated SDs were within 10% for each presented datapoint. All given concentrations were final after mixing unless stated otherwise.

Rates of Nbs binding to LacY were measured as Trp-induced quenching of bimane-labeled LacY. Stopped-flow traces were recorded at an excitation wavelength of 380 nm with emission at 441–515 nm using cut-off filters (Edmund Optics).

Steady-state fluorescence emission spectra were measured at room temperature on a SPEX Fluorolog 3 spectrofluorometer (Edison) in 2.5 mL cuvette (1 × 1 cm) as previously described (15) with excitation at 380 nm (for bimane), and 650 nm (for ATTO655). Time courses were recorded at excitation/emission wavelengths 380/465 nm and 660/677 nm for bimane- and ATTO655-labeled protein, respectively.

Homology Modeling of Nb Structures. Modeling of the 3D structures of the Nbs was carried out on SWISS-Model web-based server (40, 41) using the X-ray structure of gelsolin nanobody (PDB ID code 2X1P) as a template, which has ~70% sequence identity with LacY-derived nanobodies.

ACKNOWLEDGMENTS. We thank Alison Lundqvist for the technical assistance in the preparation of the Nbs, and Balasubramanian Dhandayuthapani and Junichi Sugihara for their skillful technical assistance in purification of the nanobodies and preparation of mutants. This work was supported by NIH Grants DK51131, DK069463, and GM073210 (to H.R.K.).

1. Saier MH, Jr (2000) Families of transmembrane sugar transport proteins. *Mol Microbiol* 35(4):699–710.
2. Guan L, Kaback HR (2006) Lessons from lactose permease. *Annu Rev Biophys Biomol Struct* 35:67–91.
3. Madej MG, Kaback HR (2014) The life and times of Lac permease: Crystals ain't enough, but they certainly do help. *Membrane Transporter Function: To Structure and Beyond*, eds Ziegler C, Kraemer R, Springer Series in Biophysics: Transporters (Springer Heidelberg, Germany) Vol 17, pp 121–158.
4. Smirnova I, Kasho V, Kaback HR (2011) Lactose permease and the alternating access mechanism. *Biochemistry* 50(45):9684–9693.
5. Kaback HR, Smirnova I, Kasho V, Nie Y, Zhou Y (2011) The alternating access transport mechanism in LacY. *J Membr Biol* 239(1-2):85–93.
6. Smirnova I, et al. (2007) Sugar binding induces an outward facing conformation of LacY. *Proc Natl Acad Sci USA* 104(42):16504–16509.
7. Madej MG, Soro SN, Kaback HR (2012) Apo-intermediate in the transport cycle of lactose permease (LacY). *Proc Natl Acad Sci USA* 109(44):E2970–E2978.
8. Abramson J, et al. (2003) Structure and mechanism of the lactose permease of *Escherichia coli*. *Science* 301(5633):610–615.
9. Mirza O, Guan L, Verner G, Iwata S, Kaback HR (2006) Structural evidence for induced fit and a mechanism for sugar/H+ symport in LacY. *EMBO J* 25(6):1177–1183.
10. Guan L, Mirza O, Verner G, Iwata S, Kaback HR (2007) Structural determination of wild-type lactose permease. *Proc Natl Acad Sci USA* 104(39):15294–15298.
11. Chaptal V, et al. (2011) Crystal structure of lactose permease in complex with an affinity inactivator yields unique insight into sugar recognition. *Proc Natl Acad Sci USA* 108(23):9361–9366.
12. Majumdar DS, et al. (2007) Single-molecule FRET reveals sugar-induced conformational dynamics in LacY. *Proc Natl Acad Sci USA* 104(31):12640–12645.
13. Kaback HR, et al. (2007) Site-directed alkylation and the alternating access model for LacY. *Proc Natl Acad Sci USA* 104(2):491–494.
14. Zhou Y, Guan L, Freites JA, Kaback HR (2008) Opening and closing of the periplasmic gate in lactose permease. *Proc Natl Acad Sci USA* 105(10):3774–3778.
15. Smirnova I, Kasho V, Sugihara J, Kaback HR (2009) Probing of the rates of alternating access in LacY with Trp fluorescence. *Proc Natl Acad Sci USA* 106(51):21561–21566.
16. Nie Y, Kaback HR (2010) Sugar binding induces the same global conformational change in purified LacY as in the native bacterial membrane. *Proc Natl Acad Sci USA* 107(21):9903–9908.
17. Kumar H, et al. (2014) Structure of sugar-bound LacY. *Proc Natl Acad Sci USA* 111(5):1784–1788.
18. Smirnova I, Kasho V, Sugihara J, Kaback HR (2011) Opening the periplasmic cavity in lactose permease is the limiting step for sugar binding. *Proc Natl Acad Sci USA* 108(37):15147–15151.
19. Smirnova I, Kasho V, Kaback HR (2014) Real-time conformational changes in LacY. *Proc Natl Acad Sci USA* 111(23):8440–8445.
20. Smirnova I, Kasho V, Sugihara J, Kaback HR (2013) Trp replacements for tightly interacting Gly-Gly pairs in LacY stabilize an outward-facing conformation. *Proc Natl Acad Sci USA* 110(22):8876–8881.
21. Fersht A (1999) *Structure and Mechanism in Protein Science: A Guide to Enzyme Catalysis and Protein Folding* (W. H. Freeman, New York), pp xxi, 631 pp.
22. Viitanen P, Garcia ML, Kaback HR (1984) Purified reconstituted lac carrier protein from *Escherichia coli* is fully functional. *Proc Natl Acad Sci USA* 81(6):1629–1633.
23. Rasmussen SG, et al. (2011) Crystal structure of the β2 adrenergic receptor-Gs protein complex. *Nature* 477(7366):549–555.
24. Steyaert J, Kobilka BK (2011) Nanobody stabilization of G protein-coupled receptor conformational states. *Curr Opin Struct Biol* 21(4):567–572.
25. Muyldermans S (2013) Nanobodies: Natural single-domain antibodies. *Annu Rev Biochem* 82:775–797.
26. Ring AM, et al. (2013) Adrenaline-activated structure of β2-adrenoceptor stabilized by an engineered nanobody. *Nature* 502(7472):575–579.
27. Staus DP, et al. (2014) Regulation of β2-adrenergic receptor function by conformationally selective single-domain intrabodies. *Mol Pharmacol* 85(3):472–481.
28. Pardon E, et al. (2014) A general protocol for the generation of nanobodies for structural biology. *Nat Protoc* 9(3):674–693.
29. Herzlinger D, Viitanen P, Carrasco N, Kaback HR (1984) Monoclonal antibodies against the *lac* carrier protein from *Escherichia coli*. 2. Binding studies with membrane vesicles and proteoliposomes reconstituted with purified *lac* carrier protein. *Biochemistry* 23(16):3688–3693.
30. Kaback HR (1971) Bacterial membranes. *Methods in Enzymology*, eds Kaplan NP, Jakoby WB, Colowick NP (Elsevier, New York), Vol XXII, pp 99–120.
31. Short SA, et al. (1974) Determination of the absolute number of *Escherichia coli* membrane vesicles that catalyze active transport. *Proc Natl Acad Sci USA* 71(12):5032–5036.
32. Owen P, Kaback HR (1978) Molecular structure of membrane vesicles from *Escherichia coli*. *Proc Natl Acad Sci USA* 75(7):3148–3152.
33. Owen P, Kaback HR (1979) Antigenic architecture of membrane vesicles from *Escherichia coli*. *Biochemistry* 18(8):1422–1426.
34. Owen P, Kaback HR (1979) Immunochemical analysis of membrane vesicles from *Escherichia coli*. *Biochemistry* 18(8):1413–1422.
35. Wu J, Kaback HR (1994) Cysteine 148 in the lactose permease of *Escherichia coli* is a component of a substrate binding site. 2. Site-directed fluorescence studies. *Biochemistry* 33(40):12166–12171.
36. He MM, Kaback HR (1997) Interaction between residues Glu269 (helix VIII) and His322 (helix X) of the lactose permease of *Escherichia coli* is essential for substrate binding. *Biochemistry* 36(44):13688–13692.
37. Mansoor SE, Farrens DL (2004) High-throughput protein structural analysis using site-directed fluorescence labeling and the bimane derivative (2-pyridyl)dithiobimane. *Biochemistry* 43(29):9426–9438.
38. Mansoor SE, Dewitt MA, Farrens DL (2010) Distance mapping in proteins using fluorescence spectroscopy: The tryptophan-induced quenching (TrIQ) method. *Biochemistry* 49(45):9722–9731.
39. Smirnova IN, Kasho V, Kaback HR (2008) Protonation and sugar binding to LacY. *Proc Natl Acad Sci USA* 105(26):8896–8901.
40. Biasini M, et al. (2014) SWISS-MODEL: Modelling protein tertiary and quaternary structure using evolutionary information. *Nucleic Acids Res* 42(Web Server issue):W252–W258.
41. Guex N, Peitsch MC, Schwede T (2009) Automated comparative protein structure modeling with SWISS-MODEL and Swiss-PdbViewer: A historical perspective. *Electrophoresis* 30(Suppl 1):S162–S173.

Supporting Information

Smirnova et al. 10.1073/pnas.1422265112

SI Methods

Materials. Oligonucleotides were synthesized by Integrated DNA Technologies. Restriction enzymes were purchased from New England Biolabs. The QuikChange II kit was purchased from Stratagene. TDG was obtained from Carbosynth Limited, NPG, D-lactose, and ATTO 655-maleimide were from Sigma. Bimane-C3-maleimide was from Life Technologies. Talon superflow resin was purchased from BD Clontech. Octyl-galactoside (OG) and DDM was from Anatrace. Synthetic phospholipids 1-palmitoyl-2-oleoyl-*sn*-glycero-3-phosphoethanolamine (POPE) and 1-palmitoyl-2-oleoyl-sn-glycero-3-phospho-(1′-rac-glycerol) (POPG) were from Avanti Polar Lipids. All other materials were of reagent grade obtained from commercial sources.

Preparation of Membrane Vesicles. RSO membrane vesicles were prepared by osmotic lysis from T184 *Escherichia coli* containing WT LacY was as described previously (1, 2) The vesicles were suspended in 100 mM potassium phosphate (KP_i)/10 mM $MgSO_4$ (pH 7.2) at a protein concentration 20 mg/mL, flash-frozen in liquid nitrogen, and stored at −80 °C until use.

Transport Assay. RSO vesicles were adjusted to an OD_{600} of 10 (10 mg of total protein per milliliter) and 50-μL aliquots were pre-incubated with 80 μg of each Nb (equivalent to ∼fivefold molar excess of Nb over LacY) at room temperature for 20 min. Lactose accumulation was assayed at given times by rapid filtration after addition of 20 mM ascorbate/0.2 mM phenazine methosulfate and 0.4 mM [1-^{14}C]lactose (10 mCi/mmol) under oxygen, as described previously (3).

Construction of Mutants, Purification of LacY, and Reconstitution into Proteoliposomes. Construction of mutants, expression in *E. coli* and purification of LacY were performed as described previously (4). All proteins contained a C-terminal 6 His-tag that was used for metal-affinity chromatography with a Talon resin. Purified proteins (10–15 mg/mL) in 50 mM sodium phosphate (NaP_i/0.02% DDM, pH 7.5) were frozen in liquid nitrogen and stored at −80 °C until use. Reconstitution into PLs was carried out with synthetic phospholipids (POPE/POPG ratio 3:1) by using the dilution method (5, 6). Briefly, purified LacY in 0.02% DDM was mixed with phospholipids dissolved in 1.2% OG maintaining a lipid:protein ratio 5:1 (wt/wt). The mixture was kept on ice for 20 min and then quickly diluted 50 times in 50 mM NaP_i buffer (pH 7.5). The PLs were collected by centrifugation for 1 h at 100,000 × *g*, suspended in the same buffer, and subjected to two cycles of freeze-thaw/sonication before use.

Labeling of LacY with Maleimide-Based Fluorophores. Purified WT LacY with Cys residues introduced on periplasmic or cytoplasmic side [50 μM protein in 50 mM NaP_i/0.02% DDM (pH 7.5) containing 5 mM TDG to protect native Cys148 from labeling] was mixed with a 1.2- to 1.5-fold molar excess of bimane-maleimide or ATTO 655-maleimide and incubated for 30 min at room temperature. Unbound fluorophores and TDG were removed by buffer exchange 2-times with 50 mM NaP_i/0.02% DDM (pH 7.5) using an Amicon Ultra-15 centrifugal filter device with 50-kDa cutoff (EMD Millipore).

1. Kaback HR (1971) Bacterial Membranes. *Methods in Enzymol*, eds Kaplan NP, Jakoby WB, Colowick NP (Elsevier, New York), Vol XXII, pp 99–120.
2. Short SA, Kaback HR, Kohn LD (1975) Localization of D-lactate dehydrogenase in native and reconstituted *Escherichia coli* membrane vesicles. *J Biol Chem* 250(11): 4291–4296.
3. Konings WN, Barnes EM, Jr, Kaback HR (1971) Mechanisms of active transport in isolated membrane vesicles. 2. The coupling of reduced phenazine methosulfate to the concentrative uptake of β-galactosides and amino acids. *J Biol Chem* 246(19):5857–5861.
4. Smirnova I, et al. (2007) Sugar binding induces an outward facing conformation of LacY. *Proc Natl Acad Sci USA* 104(42):16504–16509.
5. Newman MJ, Foster DL, Wilson TH, Kaback HR (1981) Purification and reconstitution of functional lactose carrier from *Escherichia coli*. *J Biol Chem* 256(22):11804–11808.
6. Viitanen P, Newman MJ, Foster DL, Wilson TH, Kaback HR (1986) Purification, reconstitution, and characterization of the lac permease of *Escherichia coli*. *Methods Enzymol* 125:429–452.

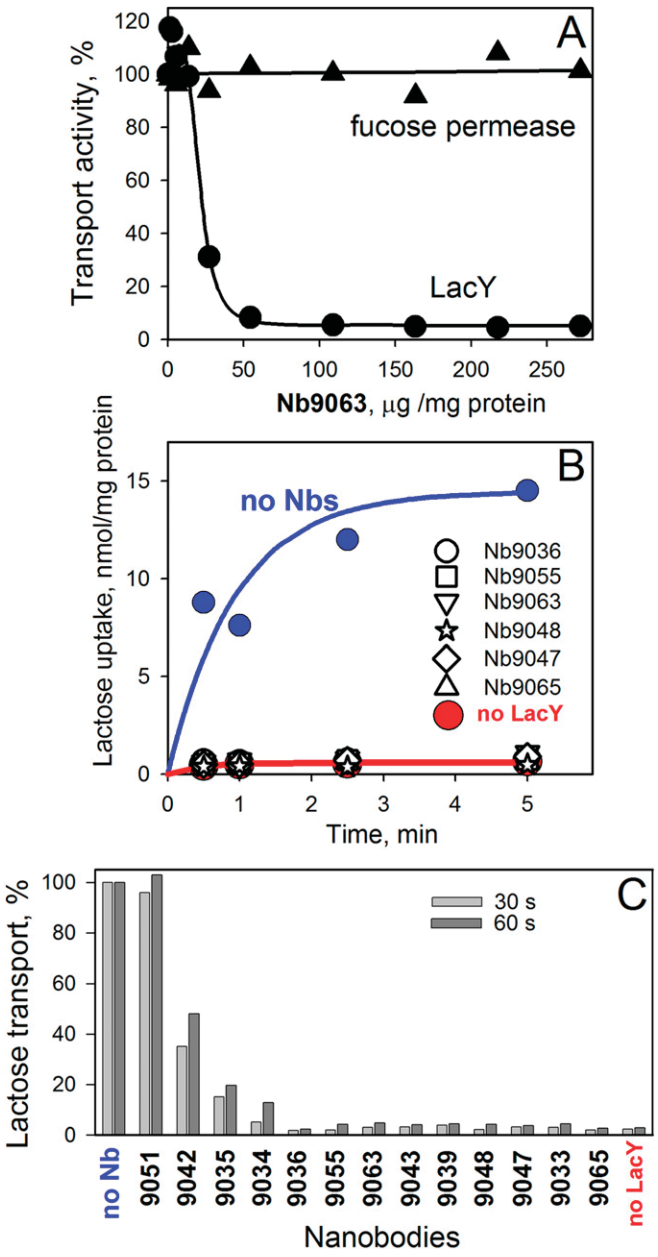

Fig. S1. Effect of Nbs on lactose transport by WT LacY. Experiments were carried out as described in *SI Methods*. (*A*) Inhibition of lactose transport by increasing concentrations of Nb 9063. Accumulation of lactose (0.5 min) was measured after preincubation of RSO vesicles (500 μg total membrane protein) containing WT LacY with the indicated amount of Nb 9063 (circles). In control experiments (triangles), uptake of [^{3}H]fucose (0.4 mM) by RSO vesicles containing FucP was measured after preincubation of vesicles with the same concentrations of Nb 9063. (*B*) Time courses of lactose accumulation by RSO vesicles containing WT LacY after preincubation with the indicated Nbs (300 μg Nb/mg membrane protein, black symbols) or without addition of Nb (blue circles). Control RSO vesicles did not contain LacY (red circles). (*C*) Transport of lactose measured with RSO vesicles containing WT LacY preincubated with indicated Nbs (300 μg Nb/mg membrane protein). Two time points (30 and 60 s) for transport are shown for each experiment. Data are expressed as percentage of lactose transport in the absence of Nb, averaged, and presented in Table 1.

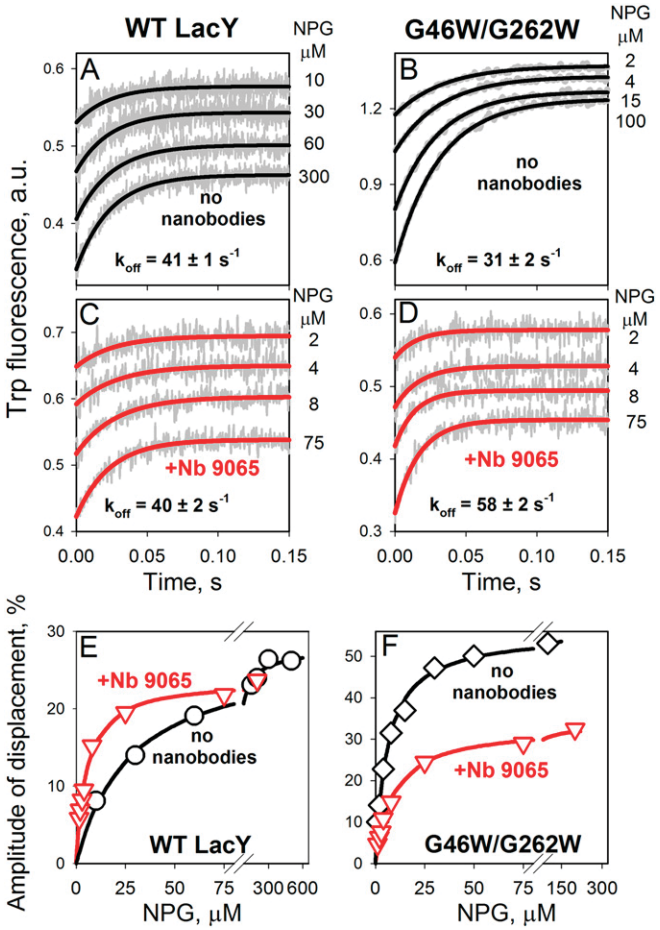

Fig. S2. Effect of Nb 9065 on kinetic parameters of NPG binding to WT LacY and mutant G46W/G262W. Affinity for NPG (K_d) and k_{off} values were determined using Trp151→NPG FRET in displacement experiments with WT LacY (*Left*) and mutant G46W/G262W (*Right*) by mixing a saturating concentration TDG (15 mM) with a protein solution containing indicated concentrations of NPG. Stopped-flow traces of Trp fluorescence increase were recorded in the absence of Nb (*A* and *B*) or with LacY preincubated with a 1.2 molar excess of Nb 9065 (*C* and *D*). Single exponential fits to the data without Nb (black lines) yield estimated k_{off} values of 41 and 31 s^{-1} for the WT and mutant, respectively. Single exponential fits to the data in the presence of Nb (red lines) yield estimated k_{off} values 40 and 58 s^{-1} for the WT and mutant, respectively. NPG binding affinity was determined from hyperbolic fits of concentration dependence of the fluorescence changes at each NPG concentration in the stopped-flow traces recorded in the absence (black lines) or presence (red lines) of Nb 9065 (*E* and *F*). The fluorescence change at each NPG concentration (amplitude of displacement) is expressed as percentage of final fluorescence level in the stopped-flow trace. The affinity of WT LacY for NPG increases in the presence of Nb 9065 (K_d decreases from 28 ± 2 to 5.3 ± 0.3 μM), whereas the K_d for mutant G46W/G262W in complex with Nb 9065 changes only slightly (from 6.1 ± 0.4 to 9.1 ± 0.5 μM). The values of k_{on} calculated from displacement experiments ($k_{on} = k_{off}/K_d$) in the presence of Nb are 7.5 and 6.4 $\mu M^{-1} \cdot s^{-1}$ for WT and mutant, respectively.

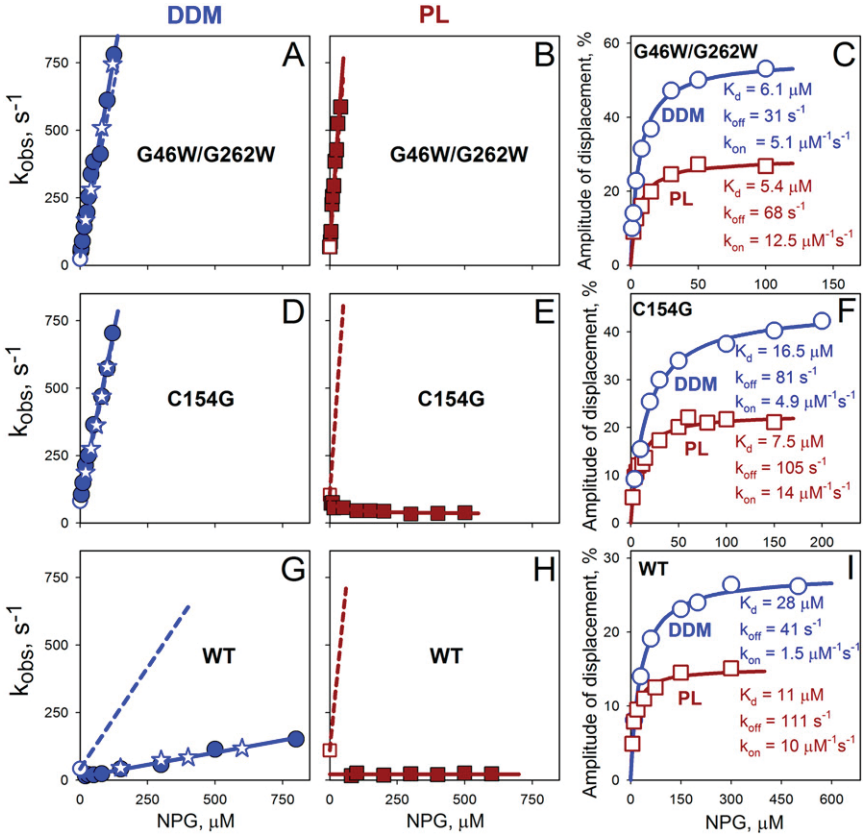

Fig. S3. Accessibility of the sugar-binding site in LacY from periplasmic or cytoplasmic side. NPG binding was measured by Trp151→NPG FRET with mutants G46W/G262W (*A*–*C*), C154G (*D*–*F*), or WT LacY (*G*–*I*) either solubilized in DDM or reconstituted into PLs. Stopped-flow rates were measured by mixing indicated concentrations of NPG with 0.5–0.8-μM proteins in DDM solution (*A*, *D*, and *G*, blue circles), in reconstituted PLs (*B*, *E*, and *H*, brown squares), or after dissolving the PLs in DDM (*A*, *D*, and *G*, stars). The linear concentration dependencies of the NPG binding rates ($k_{obs} = k_{off} + k_{on}$[NPG]) measured in DDM (*A*, *D*, and *G*) give estimates of k_{on} values (slope of the solid blue line) for G46W/G262W (5.7 $\mu M^{-1}\cdot s^{-1}$), C154G (5.0 $\mu M^{-1}\cdot s^{-1}$), and WT LacY (0.2 $\mu M^{-1}\cdot s^{-1}$). Mutant G46W/G262W reconstituted into PLs exhibits a linear concentration dependence of binding rates (*B*) (k_{on} = 5.0 $\mu M^{-1}\cdot s^{-1}$), whereas C154G and WT LacY bind sugar with constant rates independent of NPG concentration (*E*: k_{obs} = 50 and *H*: 21 s^{-1}, respectively). Dissolving the PLs in DDM results in NPG binding rates similar to those observed in DDM before reconstitution (*A*, *D*, and *G*, stars). Displacement experiments (as described in Fig. S2) were carried out with the same proteins in DDM or reconstituted into PLs. The concentration dependencies of the amplitudes of the fluorescence changes (*C*, *F*, and *I*) allow estimation of K_d values in DDM (open circles) or in PLs (open squares). The rate of displacement is a true k_{off} and does not depend on NPG concentration. Therefore, k_{on} values were calculated using measured K_d and displacement rates ($k_{on} = k_{off}/K_d$). Kinetic parameters of NPG binding obtained in displacement experiments are shown in blue or brown for data obtained in DDM and PLs, respectively. NPG binding rates with k_{on} values calculated from displacement are presented as linear concentration dependencies for comparison (broken lines in panels *A*, *B*, *D*, *E*, *G*, and *H*). The sharp slope of the linear concentration dependence of observed rates with high k_{on} value (5–14 $\mu M^{-1}\cdot s^{-1}$) indicates free access for sugar to the binding site of LacY.

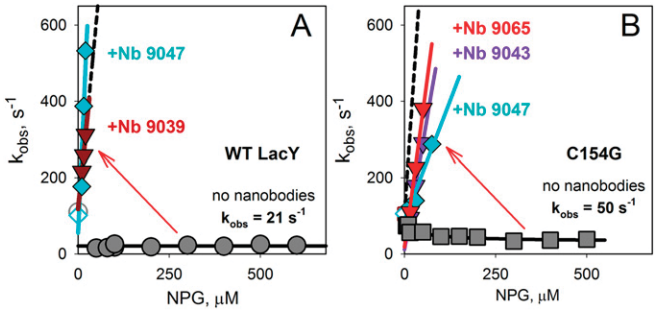

Fig. S4. Effect of Nbs on accessibility of sugar-binding site in reconstituted LacY. Sugar binding rates were measured directly as Trp151→NPG FRET as described in Fig. 2*C*, by mixing NPG with reconstituted WT LacY (*A*) or mutant C154G (*B*) in the absence of Nbs (gray symbols) or after preincubation with a 1.2-molar excess of the indicated Nb. The red arrows indicate the change in concentration dependence of sugar binding rates due to Nb binding. (*A*) For WT LacY/Nb complexes, k_{on} values were estimated as 9.7 and 22 $\mu M^{-1}\cdot s^{-1}$ for Nbs 9039 and 9047, respectively. Sugar binding in the absence of Nb is limited by opening of periplasmic cavity (k_{obs} = 21 s^{-1}). (*B*) For C154G LacY/Nbs complexes, k_{on} values were estimated as 2.5, 5.6, and 7.1 $\mu M^{-1}\cdot s^{-1}$ for Nbs 9047, 9043, and 9065, respectively. Sugar binding in the absence of Nb (k_{obs}) is 50 s^{-1}. Measured by displacement, true k_{off} values are shown as open symbols on *y* axis. Broken lines represent the concentration dependence of rates of NPG binding to the open periplasmic cavity (k_{on} = 10 and 14 $\mu M^{-1}\cdot s^{-1}$ for WT LacY and C154G, respectively) calculated from displacement experiments with reconstituted LacY. See also Fig. S3 *E*, *F*, *H*, and *I*.

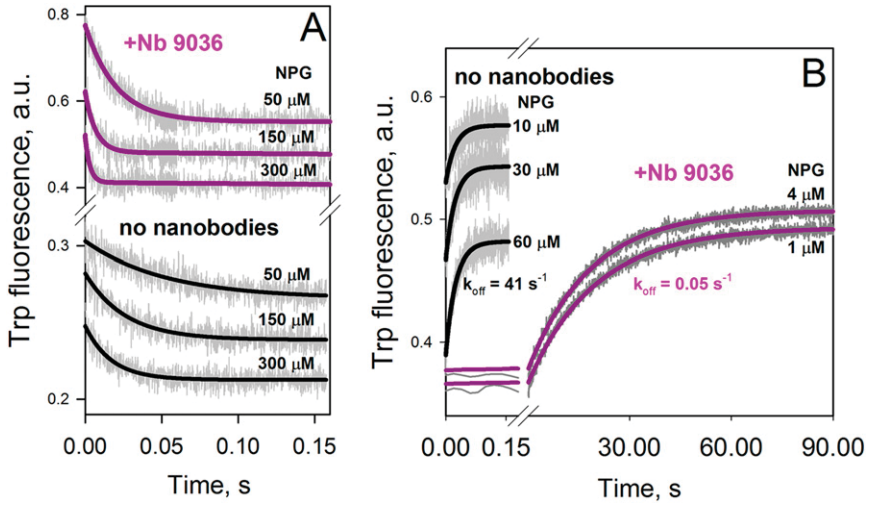

Fig. S5. Effect of Nb 9036 on sugar binding to WT LacY. NPG binding rates measured as Trp151→NPG FRET in direct binding experiments or by TDG displacement of NPG bound to LacY without Nbs or preincubated with 1.2-excess of Nb 9036. (*A*) Stopped-flow traces of Trp fluorescence decrease after mixing indicated concentrations of NPG with 0.4 μM WT LacY. The concentration dependencies of the observed rates are shown in Fig. 1*A* (black and pink lines) with estimated k_{on} = 0.2 and 1.0 $\mu M^{-1} \cdot s^{-1}$ for WT LacY and WT LacY/Nb 9036 complex, respectively (Table 1). (*B*) Stopped-flow traces of Trp fluorescence increase in displacement experiments after mixing 15 mM TDG with WT LacY (0.2 μM) preincubated with indicated concentrations of NPG. Estimated k_{off} values are 41 and 0.05 s^{-1} for WT LacY and WT LacY/Nb 9036 complex, respectively. The K_d value for NPG binding calculated from k_{off}/k_{on} is 0.05 μM for the LacY/Nb 9036 complex compared with 28 μM measured for WT LacY without Nb (Table 1).

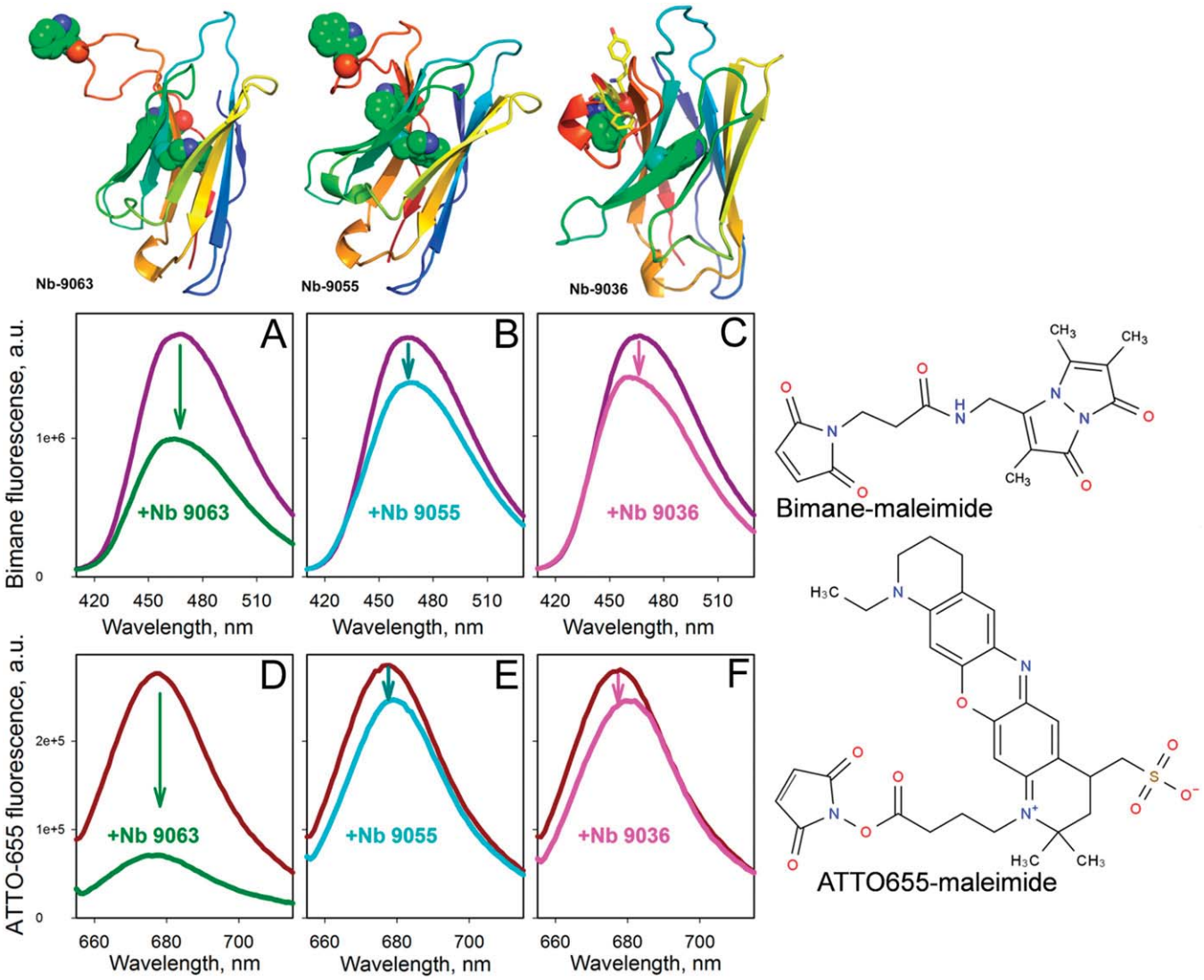

Fig. S6. Detection of Nb binding to LacY by using Trp-induced fluorescence quenching. Homology modeled structures of Nbs 9063, 9065, and 9036 are presented at the top with Trp residues shown as green spheres. Structures of bimane-maleimide and ATTO-655-maleimide fluorophores are shown on right. Fluorescence emission spectra of fluorophore-labeled mutant I32C LacY were recorded in 50 mM NaP_i/0.02% DDM (pH 7.5) before and after addition of a twofold molar excess of the indicated Nb. (*A*–*C*) Bimane emission spectra were recorded at excitation wavelength 380 nm with 0.3 μM bimane-maleimide labeled LacY. (*D*–*F*) ATTO655 emission spectra were recorded at excitation wavelength 650 nm with 0.2 μM ATTO655-maleimide labeled LacY. Arrows indicate Trp-induced fluorescence quenching in the presence of the Nb.

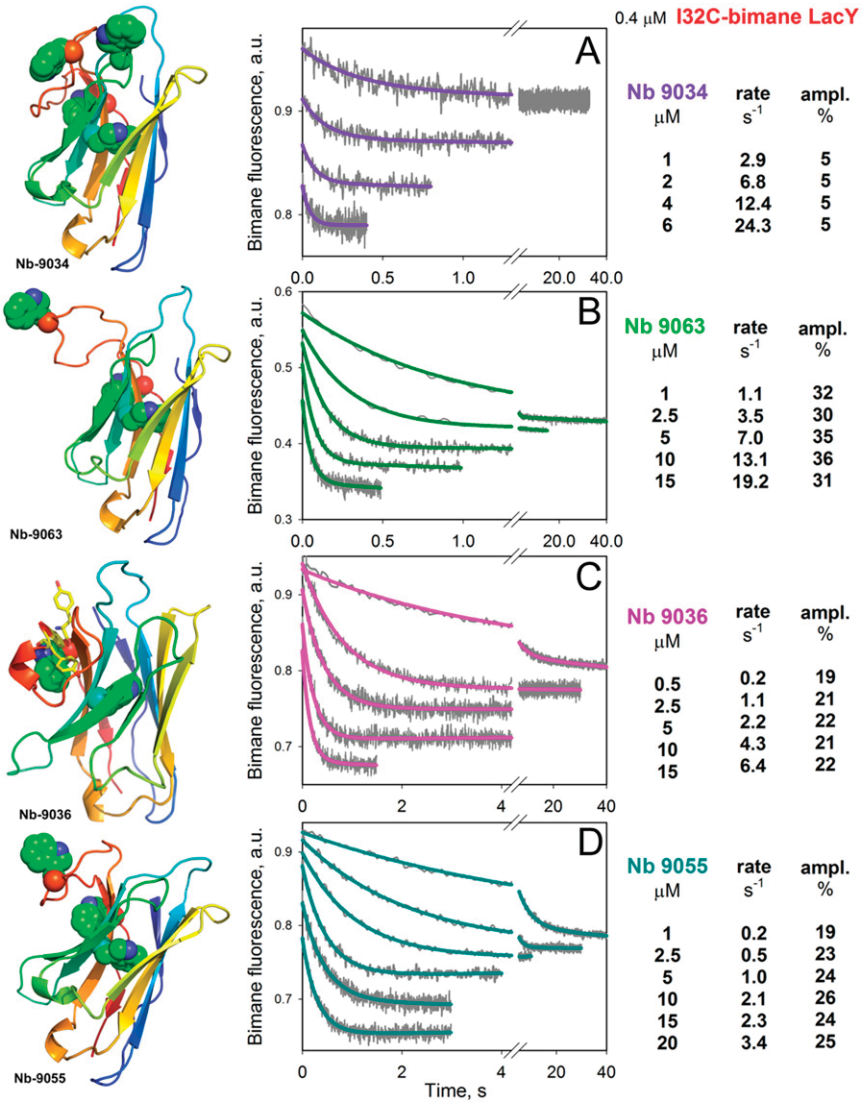

Fig. S7. Presteady-state rates of Nb binding to LacY measured as Trp-induced fluorescence quenching. Stopped-flow traces are recorded in 50 mM NaP_i/0.02% DDM (pH 7.5) after mixing bimane-labeled mutant I32C LacY (0.4 μM) with given concentrations of Nb 9034 (*A*), Nb 9063 (*B*), Nb 9036 (*C*), and Nb 9055 (*D*). Single exponential fits are shown as colored lines with estimated rates and amplitudes of the fluorescence changes given on the right. The concentration dependencies of the Nb binding rates are shown in Fig. 5. Homology models of the Nbs are shown on the left with Trp residues presented as green spheres.

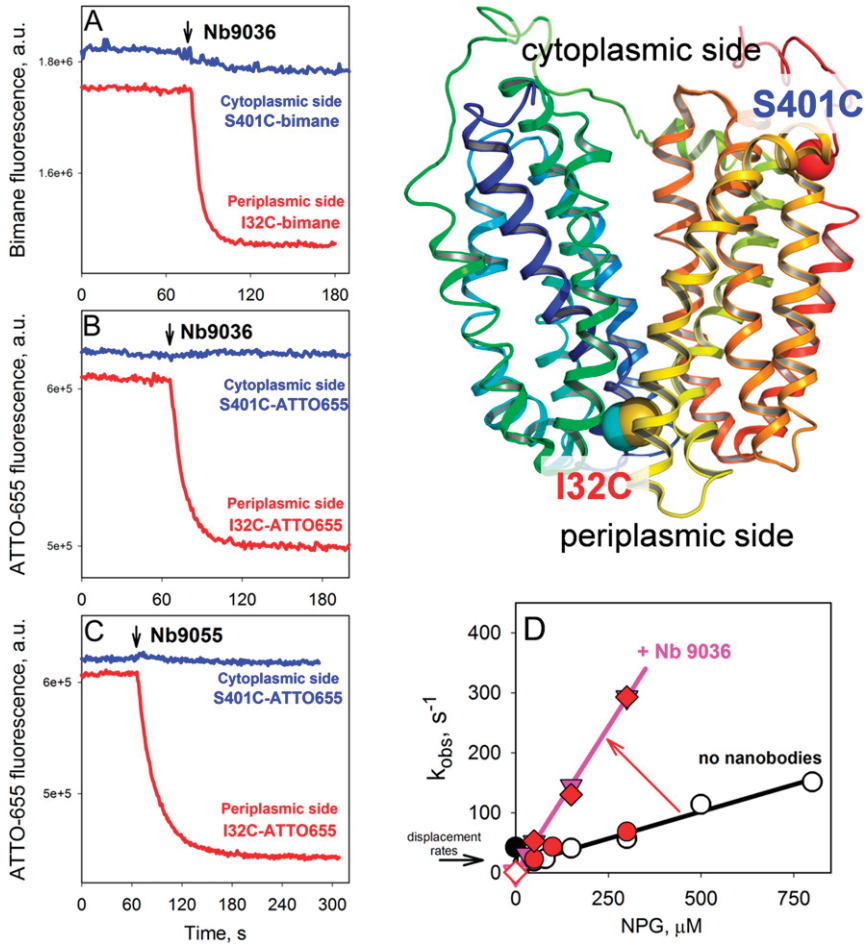

Fig. S8. Confirmation that Nb binds to the periplasmic side of WT LacY. (*A*–*C*) Cys residues introduced on periplasmic (I32C) or cytoplasmic (S401C) side of WT LacY were labeled with bimane- or ATTO655-maleimides, and the time courses of the fluorescence emission changes were recorded in 50 mM NaP_i/0.02% DDM (pH 7.5) at excitation/emission wavelengths 380/465 nm and 660/677 nm for bimane and ATTO655, respectively. The fluorescence of LacY labeled on the cytoplasmic or periplasmic sides are shown as blue or red lines, respectively. Black arrows indicate addition of 0.6 μM of a given Nb to 0.3 μM LacY labeled with bimane-maleimide (*A*) or ATTO-655-maleimide (*B* and *C*). The inward-open conformer of LacY (PDB ID code 2CFQ) with Cys replacements is shown on right. (*D*) Effect of Nb 9036 on kinetic parameters of bimane-labeled S401C mutant. The concentration dependencies of NPG binding rates were measured in the absence of Nb (filled red circles, labeled mutant S401C; open circles, WT LacY) or with Nb 9036/LacY complex (red diamonds, labeled S401C; red triangles, WT LacY). As estimated from linear fits, k_{on} values increase from 0.2 to 1.0 $\mu M^{-1} \cdot s^{-1}$ for both the WT and bimane-labeled S401C LacY complexes with Nb 9036 (see also Fig. 1). The effect of Nb 9036 on the NPG displacement rate by TDG measured with bimane-labeled S401C LacY is the same as that observed with WT LacY (k_{off} decreases from 41 to 0.05 s^{-1}, black circle and open diamond, respectively) as presented on Fig. S5*B*.

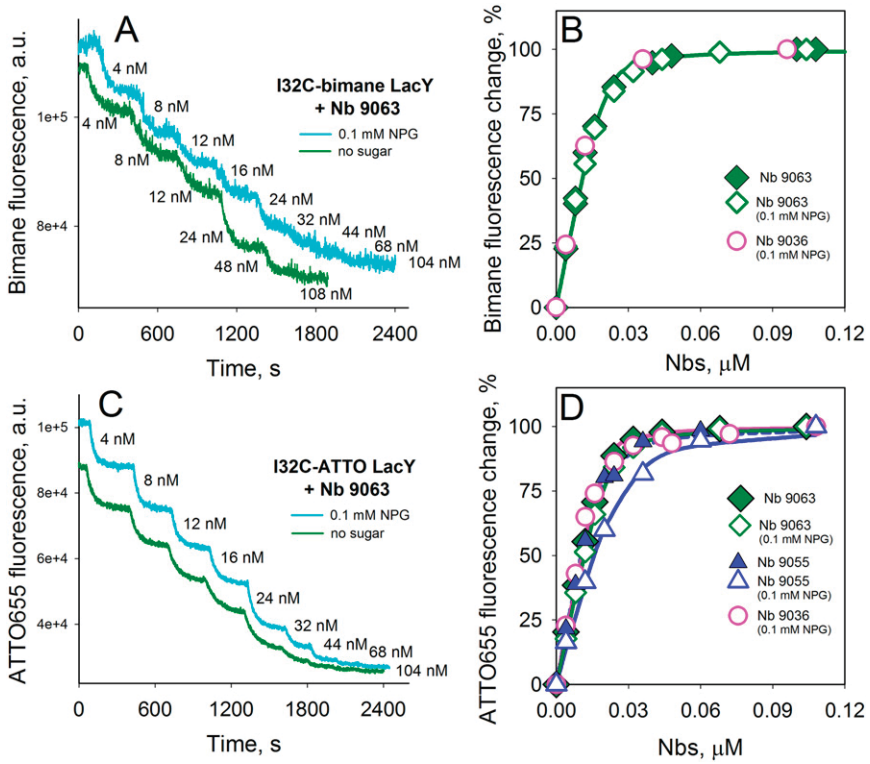

Fig. S9. Nb binding affinity. Fluorophore-labeled I32C LacY (20 nM in 2.5 mL of 50 mM NaPi/0.02% DDM pH 7.5) was titrated with Nbs 9063, 9055 or 9036. (*A* and *B*) Nbs binding to bimane-labeled LacY. (*C* and *D*) Nbs binding to ATTO655-labeled LacY. Measurements were done as described in Fig. 4. (*A* and *C*) Time courses of fluorescence quenching after sequential additions (1–3 μL) of increasing concentrations of Nb 9063 (total amount of added Nb is shown). Titrations were done at 0.1 mM NPG or without added sugar (green and cyan lines, respectively). Note slow binding rates because of low concentrations of LacY and Nb. (*B* and *D*) Concentration dependencies of the fluorescence change because of binding of the indicated Nb to labeled LacY. Fluorescence changes are expressed as percent of total fluorescence quenching in each experiment: $100(F_0 - F_{Nb})/(F_0 - F_{Nb\ max})$, where F_0 is fluorescence level without Nb; F_{Nb} is fluorescence level at indicated Nb concentration; $F_{Nb\ max}$ is final level of fluorescence at saturating Nb concentration. Data are fitted with an equation derived from equilibrium $K_d = [Nb]_{free}[P]_{free}/[Nb^{\bullet}P]$, where $[Nb^{\bullet}P]$ is a concentration of Nb/LacY complex, and $[Nb]_{free}$ and $[P]_{free}$ are concentrations of unbound Nb and LacY. Final equation used for fitting is: $f = 100((Nb + P + K_d)/2 - (((Nb + P + K_d)^2 - (4Nb^{\bullet}P))^{0.5})/2)/P$, where concentrations of Nb and LacY are total (in micromolars). Estimated K_d values are: 0.9 ± 0.2 nM for binding Nb 9063 and Nb 9036 to bimane-labeled LacY (*B*, green line); 0.9 ± 0.2 nM and 0.6 ± 0.3 nM for binding Nb 9063 and Nb 9036 to ATTO-labeled LacY (*D*, green and pink lines, respectively); and 1.6 ± 0.3 nM and 2.8 ± 0.7 nM for binding Nb 9055 to ATTO-labeled LacY in the absence or presence of sugar (*D*, broken and solid blue lines, respectively).